Andrzej ANDRZEJEWSKI

Bialystok University of Technology

doi:10.15199/48.2020.01.31

The Load Torque Influence on Time-Optimal Position Control Process

Abstract. *The contribution of the paper is the theoretical development and obtaining the time-optimal position control process in conditions of heavy loading of the servo motor as a result of simulation tests. The influence of passive load torque and active load torque on the position controller output signal generation in its active state is described mathematically.*

Streszczenie. *Wkładem pracy jest opracowanie teoretyczne oraz uzyskanie optymalno-czasowego procesu regulacji położenia w warunkach silnego obciążenia silnika serwo w wyniku badań symulacyjnych. Opisano matematycznie wpływ pasywnego momentu obciążenia oraz aktywnego momentu obciążenia na sposób generowania sygnału wyjściowego regulatora położenia w jego stanie aktywnym. (**Wpływ momentu obciążenia na minimalno-czasowy proces regulacji położenia**).*

Keywords: position control, dynamic programming, servo-drives, DC motor.
Słowa kluczowe: regulacja położenia, programowanie dynamiczne, serwonapędy, silnik prądu stałego.

Introduction

Users expect high performance [1, 2] from servo-drives not only in the steady state of their operation, but also in the transient state. The quality of the position control process in the transient state highly depends on the load torque [3]. The load torque influences the motor acceleration and deceleration in servo-drive [4]. Moreover, users expect time-optimal and without overshoot position control process not depending on the load torque character, whether it is active load torque or passive load torque [5,6,7].

Novelties of this paper are the simulation results of the optimal-time position control process without overshoot in conditions of heavy passive and heavy active load torque of the servo motor.

In paper, the DC motor linear model and nonlinear DC/DC transistor converter are utilized to obtain efficient position control system. DC motor model does not simulate nonlinearities of electromagnetic subsystem of motor [8], [9] and nonlinearities of the electromechanical subsystem [10,11,12,13,14]. However, the control system is simple in practical implementation as the result of simple assumed model.

Typically, the position control system consists of three control loops: current (electromagnetic torque) control loop, speed control loop and position control loop. Typically the PI controller are applied is control systems. However, PI type speed controller [14] always causes the speed overshoot and it can not be applied. In exemplary position control system [16] the optimization algorithm based on bee colony is applied to use high frequency switching transistor inverters. However, in paper [16] transistor inverter nonlinearities and load torque existence are completely neglected. Simulation results [16] are performed in no load state of servo motor.

Therefore, the current paper contribution is the simulation of highly loaded position control system.

The information about the load torque is necessary for accurate position control of loaded servo-drive. The load torque is typically estimated and compensated by the load torque estimator [17] or electromechanical subsystem estimator [18,19]. The fast response of load torque estimator [3] allows obtaining time-optimal speed control process after rapid load torque steps.

In paper [2] the motion profile shows expected signals of position, speed and motor acceleration. In paper [1,2] maximal acceleration and maximal decelerations are the same. The current paper contribution is motion profile by simulation results containing signal of the motor voltage additionally. Furthermore, the simulation results reveal that, the maximal acceleration and the maximal deceleration are different, because of the high load and constant motor current (electromagnetic torque) in saturation state of speed controller.

The alternative sliding mode position control system [7] is resistant to load torque existence and parameters changes. However, sliding control method causes chattering effect. Therefore, the originality of this work is to develop a position control method characterized by minimal-time positioning process without overshoot and without chattering effect caused by electromagnetic torque ripples.

Paper is divided into parts. The first part attention is redirected on the fact that motor voltage consists of many step responses not depending on the shape of reference voltage. In the next part, information about mentioned fact is utilized to obtain mathematical equations for calculation the output signals of position controller during heavy servo motor loading. Next part contains simulation results that are new time-optimal profile of highly loader servo-motor.

Significant original observation

Other scientific papers describing position control process do not utilize the fact that signals of the motor current i_r, the motor speed ω and the motor position Θ are the compositions of many step responses after motor supply voltage steps.

To continue, in electrical drives, motors are typically supplied by transistor switching converters in order to decrease the energy losses in transistors. Typically, transistors are on or off. As the result, motor supply voltage u_r is equal to $+U_{DC}$ or $-U_{DC}$, according the converter structure shown in Fig.1.

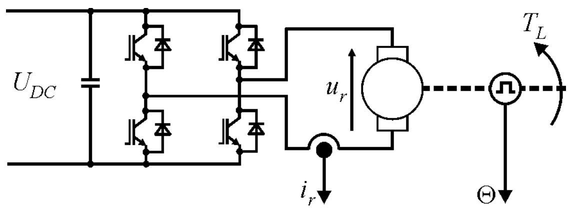

Fig.1. Structure of voltage source inverter supplying DC motor

The fact, that motor voltage is constant between switching processes, draws to conclusion that signals of motor current i_r, motor speed ω and motor position Θ can be analyzed as the composition of many step responses.

To sum up, the motor position and motor speed step responses can be utilized to overwork the new motion profile and the new position controller operation method.

The current, speed and position step responses of loaded DC motor

It is assumed that forcing motor voltage u_r is constant between switching processes:

(1) $$u_r(s) = -U_{DC}/s$$

(2) $$t_L(s) = -T_L/s$$

As the result of assumption, the motor behaviour can be analysed as a composition of many step responses. To continue, motor current signal $i_r(t)$ during motor start up can be decomposed into many motor current step responses. Motor speed signal $\omega(t)$ during motor braking can be decomposed as many speed step responses. Motor shaft position can be considered as composition of many position step responses on supply voltage steps, as follows:

(3) $$i_r(s) = \left(\left(-U_{DC} - k_M \cdot \omega(0)\right)/L_r\right) \cdot \left(1/\left((s+a)\cdot(s+b)\right)\right) + i_r(0)\cdot\left(s/\left((s+a)\cdot(s+b)\right)\right) + \left(k_M/J\right)\cdot\left(T_L/L_r\right)\cdot(1/s)\cdot\left(1/\left((s+a)\cdot(s+b)\right)\right)$$

(4) $$\omega(s) = \left(\left(-U_{DC}k_M - T_L R_r\right)/\left(L_r\, J\right)\right)\cdot\left(1/\left(s(s+a)(s+b)\right)\right) + \left(\left(k_M \cdot i_r(0) - T_L\right)/J + \omega(0)/T_r\right)\cdot\left(1/\left((s+a)\cdot(s+b)\right)\right) + \omega(0)\cdot\left(s/\left((s+a)\cdot(s+b)\right)\right)$$

(5) $$\Theta(s) = \left(\left(-U_{DC}k_M - T_L R_r\right)/\left(L_r\, J\right)\right)\cdot\left(1/\left(s^2(s+a)(s+b)\right)\right) + \left(\left(k_M \cdot i_r(0) - T_L\right)/J + \omega(0)/T_r\right)\cdot\left(1/\left(s\cdot(s+a)\cdot(s+b)\right)\right) + \omega(0)\cdot\left(1/\left((s+a)\cdot(s+b)\right)\right) + \Theta(0)/s$$

where:

(6) $$T_r = L_r/R_r$$

(7) $$a = 0.5\cdot\left(1/T_r\right)\left(1 - sqrt\left(1 - 4\left(k_M^2 L_r\right)/\left(R_r^2 J\right)\right)\right)$$

(8) $$b = 0.5\cdot\left(1/T_r\right)\left(1 + sqrt\left(1 - 4\left(k_M^2 L_r\right)/\left(R_r^2 J\right)\right)\right)$$

where: i_r – motor current (A), ω – motor angular speed (rad/s), Θ – motor angular position (rad), T_L– value of motor load torque (Nm), U_{DC} – value of converter capacitor voltage supplying transistors, H - bridge (V), R_r – motor armature winding resistance (Ω), L_r – motor armature winding inductance (H), T_r – motor armature winding time constant (s), k_M – excitation coefficient (Nm/A), J – equivalent moment of inertia (kg·m^2), $i_r(0)$ – initial condition of current step response (A), $\omega(0)$ – initial condition of angular speed step response (rad/s), $\Theta(0)$ – initial condition of angular position step response (rad).

Exact solution of step responses

The three possible step responses characters can be expected depending on the relationship between electromagnetic time constant T_r and electromechanical time constant T_M of DC motor:

(9) $$T_M = \left(J\cdot R_r\right)/k_M^2$$

The non-periodical step responses happens when electromechanical time constant T_M is greater than value $4T_r$ and as the result "a" and "b" are real and different:

(10) $$i_r(t) = A_{1NP}\cdot exp(-a\cdot t) + A_{2NP}\cdot exp(-b\cdot t) + A_{3NP}$$

(11) $$\omega(t) = B_{1NP}\cdot exp(-a\cdot t) + B_{2NP}\cdot exp(-b\cdot t) + B_{3NP}$$

(12) $$\Theta(t) = C_{1NP}\cdot exp(-a\cdot t) + C_{2NP}\cdot exp(-b\cdot t) + C_{3NP} + C_{4NP}\cdot t + \Theta(0)$$

where: A_{1NP}, A_{2NP}, A_{3NP}, B_{1NP}, B_{2NP}, B_{3NP}, C_{1NP}, C_{2NP}, C_{3NP}, C_{4NP} are constants depending on motor parameters and initial values of motor current $i_r(0)$, motor speed $\omega(0)$ and motor position $\Theta(0)$.

The non-periodical critical step responses happens when the electromechanical time constant T_M is equal to value $4T_r$ and as the result "a" and "b" are real and equal:

(13) $$a = b = 0.5\cdot\left(R_r/L_r\right)$$

(14) $$i_r(t) = A_{1C}\cdot t\cdot exp(-a\cdot t) + A_{2C}\cdot exp(-a\cdot t) + A_{3C}$$

(15) $$\omega(t) = B_{1C}\cdot t\cdot exp(-a\cdot t) + B_{2C}\cdot exp(-a\cdot t) + B_{3C}$$

(16) $$\Theta(t) = C_{1C}\cdot exp(-a\cdot t) + C_{2C}\cdot t\cdot exp(-a\cdot t) + C_{3C} + C_{4C}\cdot t + \Theta(0)$$

in which A_{1C}□, A_{2C}, A_{3C}, B_{1C}, B_{2C}, B_{3C}, C_{1C}, C_{2C}, C_{3C} are constants.

The periodical step response happens when electromechanical time constant T_M is smaller than value $4T_r$ and as the result "a" and "b" are complex:

(17) $$a = \sigma + j\omega_0$$

(18) $$b = \sigma - j\omega_0$$

(19) $$\sigma = 0.5\cdot\left(R_r/L_r\right)$$

(20) $$\omega_0 = 0{,}5\cdot\left(R_r/L_r\right)\cdot sqrt\left(\left(4\cdot k_M^2\cdot L_r\right)/\left(R_r^2\cdot J\right) - 1\right)$$

(21) $$i_r(t) = A_{1P}\cdot\exp(-\sigma\cdot t)\cdot\sin(\omega_0 t) + A_{2P}\cdot\exp(-\sigma\cdot t)\cdot\cos(\omega_0 t) + A_{3P}$$

(22) $$\omega(t) = B_{1P}\cdot\exp(-\sigma\cdot t)\cdot\sin(\omega_0 t) + B_{2P}\cdot\exp(-\sigma\cdot t)\cdot\cos(\omega_0 t) + B_{3P}$$

(23) $$\Theta(t) = C_{1P}\cdot\exp(-\sigma\cdot t)\cdot\sin(\omega_0\cdot t) + C_{2P}\cdot\exp(-\sigma\cdot t)\cdot\cos(\omega_0\cdot t) + C_{3P} + C_{4P}\cdot t$$

where: A_{1P}, A_{2P}, A_{3P}, B_{1P}, B_{2P}, B_{3P}, C_{1P}, C_{2P}, C_{3P} are constants.

The preparation process of the equation describing position controller operation is not finished. To continue, the exact solutions of motor current □(10□), (14), (21), speed (11), (15), (22) and position responses (12), (15), (23) can not be directly used in signal processor calculations, because computer does not calculate exact value of mathematical functions such as: exp(x), sin(x) or cos(x). The processor arithmetic unit calculates only three mathematical operations such as: addition, subtraction and multiplication. Therefore it is justified to develop all equations describing step responses into Maclaurin series.

Approximation of motor current, motor speed and motor position step responses

Mathematical equations describing motor current $i_r(t)$, motor speed $\omega(t)$ and motor position $\Theta(t)$ step responses are prepared for digital signal processor operations by expansion them into Maclaurin series:

(24) $$f(t) = f'(0) + f''(0)\cdot t + 0.5\cdot f'''(0)\cdot t^2 + \ldots$$

(25) $$i_r(t) = -\left(\left(U_{DC} + k_M\cdot\omega(0) + R_r\cdot i_r(0)\right)/L_r\right)\cdot t + i_r(0)$$

(26) $$\omega(t) = -0{,}5\left(k_M/J\right)\left(\left(U_{DC} + k_M\omega(0) + R_r i_r(0)\right)/L_r\right)\cdot t^2 + \left(k_M/J\right)\cdot\left(i_r(0) - \left(T_L/k_M\right)\right)\cdot t + \omega(0)$$

(27) $$\Theta(t) = -(1/6)\left(k_M/J\right)\left(\left(U_{DC} + k_M\omega(0) + R_r i_r(0)\right)/L_r\right)\cdot t^3$$

$$+0.5\cdot\left(k_M/J\right)\cdot\left(i_r(0)-\left(T_L/k_M\right)\right)\cdot t^2+\omega(0)\cdot t+\Theta(0)$$

By analysis of equations (24), (25) and (27) we can come the conclusion that approximated description of motor current, motor speed and motor position step responses are the same not depending the character of step responses, whether step responses are non-periodical (10), (11), (12) or non-periodical critical (14), (15), (16) or periodical (20), (21), (22).

Formula describing position control error $\Delta\Theta$ is obtained under condition that the signal of the reference position is constant:

$$\Delta\Theta(t)=\Theta_{ref}-\Theta(t) \tag{28}$$

$$\Delta\Theta(t)=(1/6)\left(k_M/J\right)\left(\left(U_{DC}+k_M\omega(0)+R_r i_r(0)\right)/L_r\right)\cdot t^3 -0.5\cdot\left(k_M/J\right)\cdot\left(i_r(0)-\left(T_L/k_M\right)\right)\cdot t^2-\omega(0)\cdot t+\Delta\Theta(0) \tag{29}$$

In equations (25), (26) and (29) the same sets of elements exist. It is the advantage, because by using symbolic substitution the computation process needs less processor operations.

Position controller operation

Equations (25), (26) and (29) describe the position controller operation according to Bellman dynamic programming method, as it is shown in Fig.2. Position control algorithm is performed in two steps. In the first step, the equation (29) is solved in order to obtain time t. Then time is substituted to equations (25) and (26) in order to obtain reference speed ω_{ref} and reference current i_{ref}.

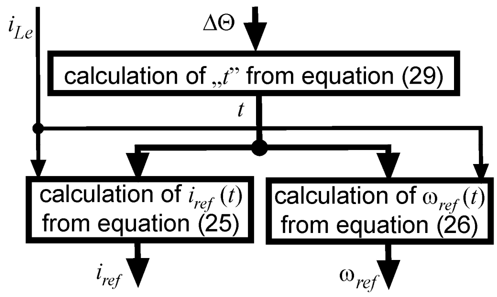

Fig.2. Generation of the output signals of position controller in the active state

It should be emphasized, that equations (25), (26) and (29) are calculated on the basis of estimated load current i_{Le} [3,18,19] which is the ratio of the load torque T_L to the excitation coefficient k_M. Therefore, the conclusion is drawn, that equations describe the influence of the passive load torque and the active load torque on the position controller output signal in its active state.

Simulation investigations

Simulation is performed for two reasons. Firstly, the idea of the dynamic programming method in conditions of heavy loading of the servo motor is verified. Secondly, non-linear position controller is created as a program and tested. Simulation investigation is performed in Matlab-Simulink software with sample time: 10ns in order to neglect the integration errors. There are assumed the following DC motor model parameters: R_r=4.65Ω, L_r=70mH, T_r=15ms, J=0.0328kgm^2, k_M=1.35Nm/A, T_M=83.68ms, T_L=0.54Nm and DC/DC converter parameters: U_{DC}=325V, I_{MAX}=5A, Ω_{MAX}=6rad/s.

Simulation results shown in Fig.3 and Fig.5 reveals that signal of motor speed has different sloped in transient state. It can be explained by the two facts existence. The first fact is that motor generates constant electromagnetic torque, because of limitation to maximal current I_{MAX}. Another fact is that the high load torque substracts form the motor electromagnetic torque and causes higher or smaller motor acceleration.

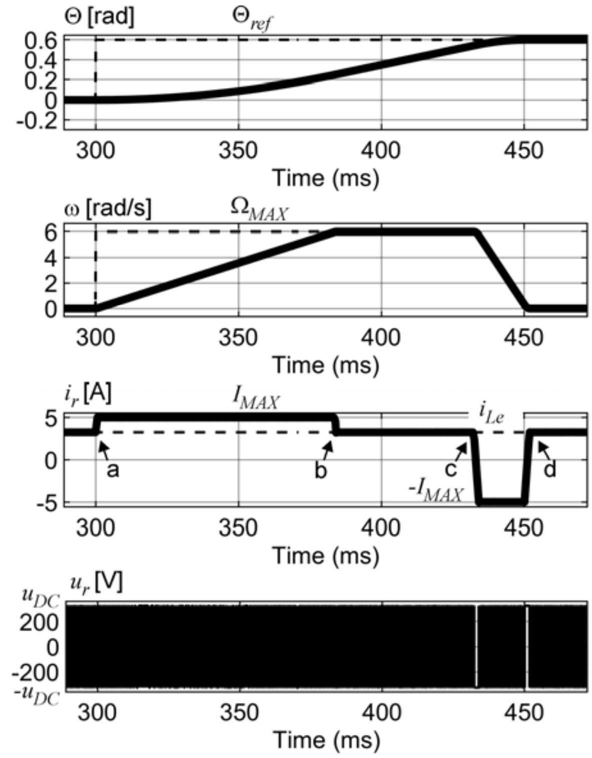

Fig.3. Motor position Θ motor speed ω, motor current i_r and motor voltage u_r during time-optimal position control process with passive load torque

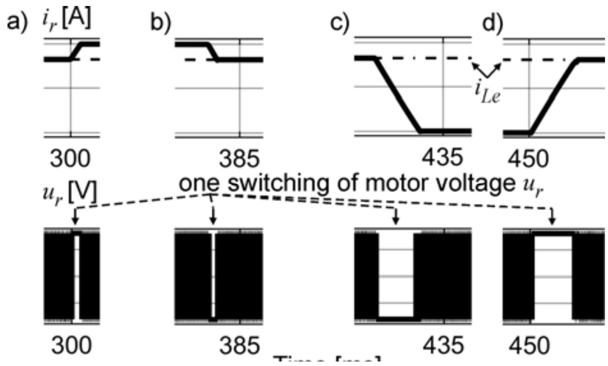

Fig.4. Signals magnification depicted in Fig.4 showing motor voltage u_r steps and motor current i_r step responses with passive load torque

Simulation results in Fig.3 and active load in Fig.5 shows the time-optimal position control process without overshoot during heavy passive load. The control process is time-optimal, because it is performed with maximal forcing motor voltage U_{DC} and maximal limitations in servo drive that is with maximal current I_{MAX} and maximal speed Ω_{MAX}. The application of maximal voltage during position control process is documented in Fig.4 and Fig.6. The passive load torque causes that the maximal voltage is applied longer in active state of position controller, in fig,4.c and Fig.4d, whereas the active load torque causes that maximal voltage is applied longer is saturation stage of position controller, in Fig.6a and Fig.6b. The documented in Fig.4d and Fig.6d, the one switching process of voltage u_r reveals the lack of position overshoot, whereas the equality of the motor current i_r to the load current i_{Le} is the evidence of the load torque compensation for zeroing position error (29).

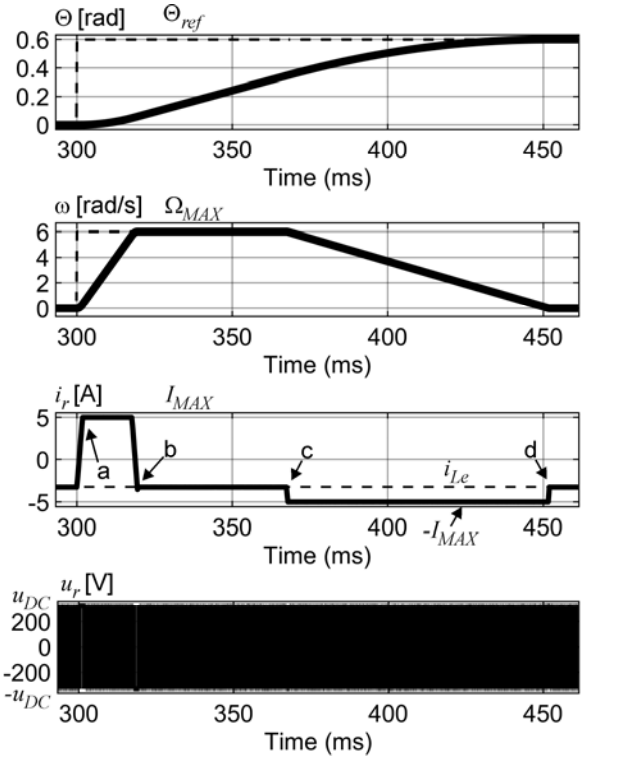

Fig.5. Motor position Θ motor speed ω, motor current i_r and motor voltage u_r during time-optimal position control process with active load torque

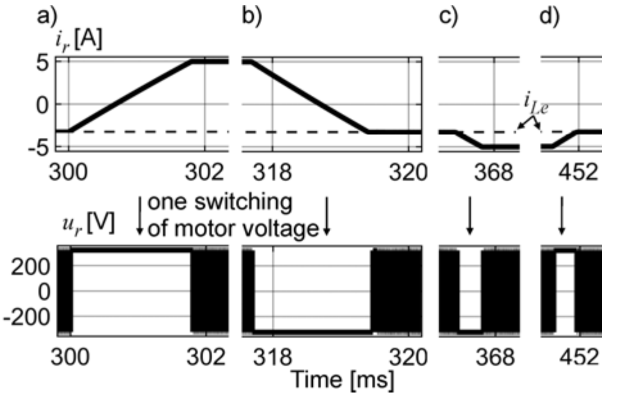

Fig.6. Signals magnification depicted in Fig.6 showing motor voltage u_r steps and motor current i_r step responses with active load torque

Conclusion

To sum, up, the new position controller is designed and the time-optimal position control process during servo motor heavy loading conditions is obtained. The passive and the active load torque influence on time-optimal position control process is visualized with simulation results and discussed. To continue, the heavy load torque causes that acceleration differs for motor deceleration during position control process. The simulation results reveal the lack of position overshoot of highly loaded servo motor.

This work was supported by Ministry of Science and Higher Education in Poland under work No. S/WE/1/2018.

Author: *dr inż. Andrzej Andrzejewski, Politechnika Białostocka, Katedra Energoelektroniki i Napędów Elektrycznych, ul. Wiejska 45A, 15-351 Białystok, E-mail: a.andrzejewski@pb.edu.pl.*

REFERENCES

[1] Bychkov M., Kuznetsova V., Optimum and quasioptimum control of the position electric drive by criterion of electric losses minimum, *25th International Workshop on Electric Drives: Optimization in Control of Electric Drives (IWED)*, (2018), 1 – 6

[2] Samygina E.K., Rassudov L., N., Balkovoi A., P., Comparison of linear position and velocity control strategies for a direct servodrive, *2018 25th International Workshop on Electric Drives: Optimization in Control of Electric Drives (IWED)*, (2018), 1-5

[3] Andrzejewski A., "Simulation investigations of time-minimal speed control process after load torque step", *Przegląd Elektrotechniczny*, 88 (2012), No. 2, 349-356

[4] Kabziński J., Adaptive Servo Control with Polynomial Approximation of Stribeck Curve, *Przegląd Elektrotechniczny,* 90 (2014), No. 5, 20-24

[5] Nourisola H., Azizi A., Majidabad S., S., Pre-Compensated Proportional Derivative Sliding Mode Controller Design for Image Based Visual Servoing, *2019 5th Conference on Knowledge Based Engineering and Innovation (KBEI)*, (2019), 725-730

[6] Samygina E.K., Enhancement of Servodrive Control System for Exact Tracking in the Extended Speed Range, *2018 X International Conference on Electrical Power Drive Systems (ICEPDS)*, (2018), 1-4

[7] Kardoš J., Synthesis of a robust control algorithm for a robot positioning, *2018 ELEKTRO*, (2018), 1 – 6

[8] Makarchuk O., Calus D., Moroz V., Gałuszkiewicz Z., Gałuszkiewicz P., Two-dimensional fem-analysis of eddy currents loss in laminated magnetic circuits, *Electrical Engineering & Electromechanics*, (2019), No. 1, 41-45

[9] Bjekic M., Sucurovic M., Bozic M., Rosic M., Antic S., Using computer for measurement and visualization of rotating magnetic field in AC machines, *Computer Applications in Engineering Education*, 25 (2017), No. 4, 608-624

[10] Popenda A., Mathematical modelling of real transmission shafts and mechanical connections with clearances, *Przegląd Elektrotechniczny*, 93 (2017), No. 1, 189 – 192

[11] Popenda A., Mathematical modelling of induction motor with a saturated magnetic circuit during changes in moment of inertia*, Przegląd Elektrotechniczny*, 91 (2015), No. 12, 202-204

[12] Czaban A., Lis M., Modelowanie matematyczne procesów nieustalonych w układzie napędowym dźwigu, *Przegląd Elektrotechniczny*, 79 (2017), No. 12, 79 – 82

[13] Serkies P., J., Predictive speed control in PMSM servo drive with elastic coupling at different blocking controls technique, *Przegląd Elektrotechniczny*, 91 (2015), No. 11, 271-274

[14] Żychlewicz M., Derugo P., Zastosowanie sterowania z modelem wewnętrznym opartego o sieci neuronowe dla napędu z elastycznym sprzęgłem, Przegląd Elektrotechniczny, 94 (2018), No. 5, 163 - 168

[15] Waluś Ł., Dubowski M., R., Badania symulacyjne adaptacyjnego obserwatora strumienia magnetycznego oraz prędkości kątowej układu napędowego z maszyną asynchroniczną, *Przegląd Elektrotechniczny*, 94 (2018), No.11 174-178

[16] Tarczewski T., Skiwski M., Grzesiak L., M., Zieliński M., Sterowanie bazujące na sprzężeniu od wektora zmiennych stanu z ograniczeniami serwonapędem z silnikiem PMSM, *Przegląd Elektrotechniczny*, 94 (2018), No. 3, 99-105

[17] Baran J., Jąderko A., Control of the wind turbine with aerodynamic torque estimation, *Przegląd Elektrotechniczny*, 94 (2018), nr 5, 47-52

[18] Andrzejewski A., Investigation into the Moment of Inertia Estimation Process Occurring in Electric Drive of a Mechatronic System, *Proceedings of the 2018 18th International Conference on Mechatronics - Mechatronika (ME),* (2018), 53 - 60

[19] Andrzejewski A., Methods for reducing the estimation error of the moment of inertia, *Przegląd Elektrotechniczny*, 94 (2018), nr 12, 100-107